Engineering Structures 148 (2017) 509–521

Contents lists available at ScienceDirect

Engineering Structures

journal homepage: www.elsevier.com/locate/engstruct

Doppler radar-derived wind field of five tornado events with application to engineering simulations

Maryam Refan [a,*], Horia Hangan [a], Joshua Wurman [b], Karen Kosiba [b]

[a] WindEEE Research Institute, The University of Western Ontario, 1151 Richmond St, London, Ontario N6A 3K7, Canada
[b] Center for Severe Weather Research, 1945 Vassar Circle, Boulder, CO 80305, USA

ARTICLE INFO

Article history:
Received 20 January 2016
Revised 3 March 2017
Accepted 27 June 2017
Available online 10 July 2017

Keywords:
Doppler radar
Tornado vortex
Velocity field
Fujita Scale

ABSTRACT

Doppler radar data corresponding to five tornado events are analyzed using the Ground-Based Velocity Track Display method and the three-dimensional velocity field of nine volumetric samples is extracted. These samples are selected to cover a range of wind speeds (between 36 m/s and 64 m/s) and vortex structures representative of EF0 to EF3 tornadoes in a first attempt to generate a tornado wind field database. Tangential velocity profiles, swirl ratios and vortex structures, i.e. single-celled or two-celled vortex, are determined for each of these volumetric samples.

Among the nine volumetric samples, two show single-celled characteristics, vortex breakdown bubble is evident in one and four demonstrate two-celled vortex characteristics. The radial profiles of the tangential velocity are in good agreement with a modified Rankine vortex model. The variation of maximum tangential velocities with height is very different when compared to the velocity variation in typical atmospheric boundary layer flows. The swirl ratios of the tornado volumetric samples are computed using the flow rate through the updrafts and the maximum circulation in the flows.

1. Introduction

The United States experiences an average of more than 1200 tornadoes per year which have resulted in around 1300 fatalities and more than $24 billion damage in the previous 15 years [1]. The damage from tornado outbreaks in 2011 exceeded $10 billion, representing the highest severe weather-related property damage in a single year since 1980 [2]. The National Institute of Standards and Technology (NIST) report [3] on the impacts of the 22 May 2011 EF5-rated Joplin, MO tornado details that a total of 553 non-residential and 7411 residential buildings were damaged to some extent with about 43 percent of the residential buildings being destroyed (i.e. damage classification of heavy/totaled or demolished). Losses from damaged buildings in this tornado, excluding damaged automobiles and other properties, totaled about $1.78 billion. While many of the affected buildings did not collapse, 84% of the total fatalities were building-related and 96% of the deaths (155 out of 161) were caused by impact–related injuries which means due to blunt force trauma.

Effectively designing tornado-resistant buildings and structures requires a detailed knowledge of the nature of the wind threat including associated flow fields, intensity, translational path and directional variability, geographical occurrence and statistics as well as debris dynamics. Characterizing the complex structure of tornado flows and simulating tornado vortices with flow characteristics similar to natural tornadoes are the main steps in achieving this long term goal. However, there are historical barriers: (i) the shortage of full-scale velocity data, (ii) the unknown relationship between actual and simulated tornadoes and (iii) the limited scale of tornado simulators.

Collecting wind field data from tornadoes in nature has been historically challenging. Technological developments of Doppler radars (e.g. introduction of Doppler On Wheels (DOW) [4]) are important recent advancements enabling full-scale tornado data collection from a safe distance. However, until now the data analysis from these measurements was mainly focused on tornadogenesis and individual events.

To ensure that experimentally or numerically simulated tornadoes have the same characteristics as field tornadoes, all the similitude requirements must be satisfied. The complexity with tornado simulations emanates from the swirl ratio (S) definition. This important controlling parameter is defined based on the geometry of a simulator and for that reason, the determination of the swirl ratio for a field tornado is difficult/subjective as inlet and outlet boundaries of a field tornado are not clearly detectable. Alternatively, Hangan and Kim [5] suggested a practical approach towards

* Corresponding author.
E-mail address: maryam.refan@uwo.ca (M. Refan).

http://dx.doi.org/10.1016/j.engstruct.2017.06.068
0141-0296/

properly scaling tornado vortices in laboratory which was further developed and verified by Refan et al. [6].

Considering the reduced size of the simulators and therefore, their small geometric scaling ratio, modeling buildings and structures and measuring the wind-induced loads has not been practical. However, the introduction of new wind facilities, such as the WindEEE Dome at Western University, enables researchers to simulate tornado vortices in laboratory at a relatively large scale and with flow characteristics similar to real tornadoes.

It is only recently that advanced techniques have emerged at the level of field characterizations (mobile Doppler radars [4]), mathematical modeling (Ground-Based Velocity Track Display [7]) and experimental simulations (novel tornado simulators [8] and lately developed scaling practices [6]). Herein we implement some of these new techniques to characterize the flow structure and velocity field of various tornado events. First, single-Doppler radar data and the Ground-Based Velocity Track Display (GBVTD) method [7] are used to extract the three-dimensional flow field of nine volumetric samples (hereafter volumes) corresponding to five tornado events. Next, the vertical structure of the tornadoes revealed in these nine volumes are compared with simulated tornado vortices. Tornado volumes are then ranked in an increasing order of Enhanced Fujita Scale (EF-Scale) [9], determined based on radar-measured maximum tangential velocity, to avoid the subjectivity in tornado intensity ranking introduced by using damage survey findings. At the end, the swirl ratio of each volume is estimated using a new approach which is based on the flow field and then is related to the EF-Scale. This analysis has the potential to build a relationship between full-scale tornado events and physically or numerically simulated tornado-like vortices. The analyzed data will serve as the beginning of what will eventually be a database of full-scale tornado wind fields. This preliminary database can be used by researchers focusing on experimental and numerical simulations of tornadic flows with the ultimate goal of studying wind-loading effects on scaled models of buildings and structures.

2. Background

Physical [10–14] and numerical [15–18] simulations of tornado-like flows have demonstrated variations in the vortex intensity, structure and wind field, which are mainly governed by the non-dimensional parameter known as the swirl ratio (S). The swirl ratio can be defined as the ratio between the tangential velocity (V_{tan}) at the edge of the updraft hole to the mean axial velocity (V_{ax}) through the updraft opening: $S = (1/2a)V_{tan}/V_{ax}$. Where a, namely the aspect ratio, is the ratio between the inflow depth (h) and the updraft radius (r_0). The terms inflow depth (a.k.a. inflow height) and updraft hole originate from Ward-type tornado simulators and are depicted in Fig. 1.

As shown in Fig. 2, variation of the swirl ratio results in various tornado structures [19]. For very weak swirls, $S < 0.2$, the flow in the boundary layer region separates (Fig. 2a). By increasing the angular momentum, a thin laminar swirling flow forms aloft while the separated flow is forced to reattach to the surface (Fig. 2b). For moderate swirls, $0.2 < S < 0.4$, a turbulent vortex breakdown bubble forms aloft and moves towards the surface as the swirl ratio increases (Fig. 2c). At this transitional stage, the vortical flow consists of a thin core close to the ground (supercritical zone) and a turbulent two-celled flow aloft (subcritical zone). By further increasing the swirl ratio, a downdraft develops along the centerline and eventually the breakdown bubble touches the surface at $S \approx 0.45$ (Fig. 2d). For $0.8 < S < 1.4$, a two-celled vortex with a central downdraft impinging on the ground is observed (Fig. 2e). The tornado vortex can split into two or more cells if the swirl increases further (Fig. 2f). As explained by Hall [20,21], a key feature of quasi-cylindrical vortices is to develop an adverse axial pressure gradient which is related to the radial expansion of the turbulent core aloft. As a result, the updraft decelerates at the centerline and maximum vertical velocities relocate to an annular ring surrounding the vortex breakdown bubble. The presence of vortex breakdowns in actual tornadoes has been confirmed by Pauley and Snow [22] and Lugt [23]. Note that the swirl ratio values and ranges provided above correspond to measurements performed in a Ward-type tornado simulator [24].

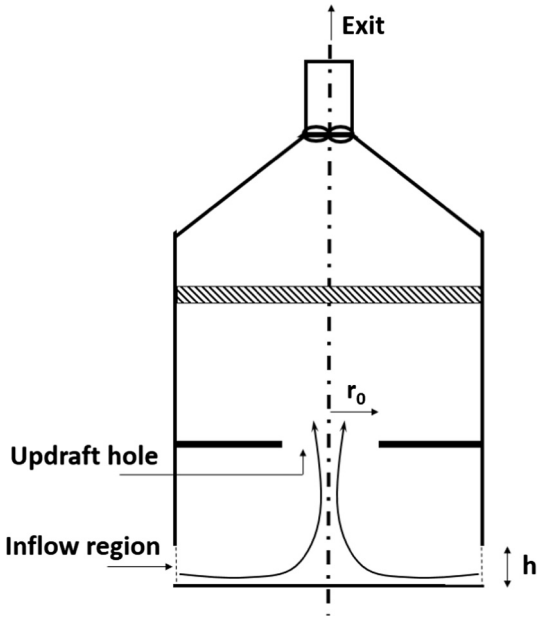

Fig. 1. Schematic drawing of a typical Ward-type tornado simualtor.

Single- and dual-Doppler radar data from over 200 individual tornadoes have been collected using proximate mobile Doppler On Wheels (DOW) radars [4,25] during field projects such as Verification of the Origins of Rotation in Tornadoes Experiment 1 (VORTEX1: 1994–1995), Radar Observations of Tornadoes And Thunderstorms Experiment (ROTATE: 1996–2001; 2003–08; 2012–13) and VORTEX2 (2009–2010). The first three-dimensional maps of a tornado vortex inner and outer core flow with fine temporal and spatial resolution were obtained using the prototype DOW mobile radar in VORTEX1 [26]. These tornado wind maps allowed for recording the horizontal and vertical structure of the vortex and its evolution [27–29]. ROTATE [30,31] collected single- and dual-Doppler radar data from more than 140 different tornadic events that enabled the study of tornadogenesis [32], tornado structure [33–37] and the relationship between tornadic winds, debris, and damage [38–40].

ROTATE (2012–13) is the most recent field study of tornadoes focused on the low-level winds and therefore of great interest for the wind engineering community. Using data collected during this field project, Kosiba and Wurman [41], for the first time, documented the fine-scale three-dimensional structure of the surface layer in a tornado.

The Ground-Based Velocity Track Display (GBVTD) technique was developed by Lee et al. [7] to resolve the wind structure of a tropical cyclone using single-Doppler radar data. The method was then extended by Lee and Wurman [35] to retrieve three-dimensional structure of tornadoes. Since then, the GBVTD method has been used by many researchers [36,37,41–46] to extract the wind field of tornadoes from single-Doppler radar measured data.

Lately, Nolan [47] performed a thorough review on the accuracy of the GBVTD method in retrieving velocity fields from single-Doppler radar data. He concluded that vertical velocities obtained

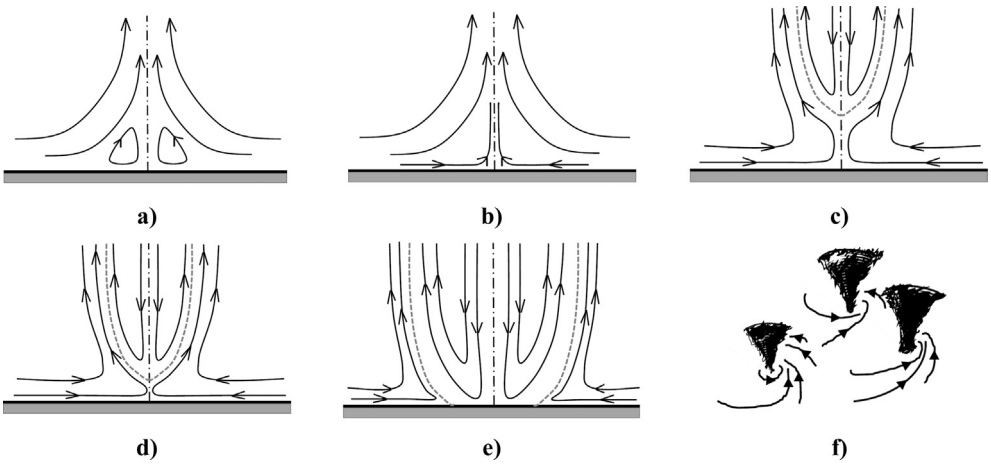

Fig. 2. Swirl ratio effect on the structure of tornado vortices; (a) very weak swirl, (b) laminar core, (c) breakdown bubble formation, (d) drowned vortex jump, (e) two-celled turbulent vortex and (f) a family of three vortices – image adapted from [19].

through this mathematical method are biased, especially in weak tornadoes. This is due to the effect of centrifuging of debris and hydrometeors at low-levels which is shown to be more pronounced for tornadoes rated F2 or less. The bias introduced to the radial velocities (and consequently the axial velocities) can be determined to some extent [47,48] given that information about the size and type of scatterers is available over the life cycle of a tornado event.

Nevertheless, retrieving the three-dimensional wind field of tornadoes is an ongoing research and improvements in the GBVTD method and in the correction for centrifuging effects are expected in the near future.

Overall the research so far has been focused on either developing the GBVTD technique or on applying it to characterize mostly singular events with meteorological applications. Herein, for the first time, GBVTD is applied to analyze, in detail, the flow structure of multiple tornadic events corresponding to various EF-Scales. An important aspect of the present study is that all the tornado events have been consistently analyzed and then inter-compared. This work can therefore form a prerequisite for building a three-dimensional flow field database for tornadoes that can be used to calibrate engineering simulations (experimental/numerical) of tornadoes. In turn, the engineering simulations can be further applied on model buildings and structures to determine tornado loading and differentiate it from straight/synoptic winds loading and therefore generate much needed building/structure design guidelines, codes and standards for tornado prone areas.

3. Data analysis

The main limiting factors in generating full-scale tornado flow database are the availability of field measurements and then the quality of the data. At this preliminary stage of developing the database, events and consequently the volumes were selected (from the data that was made available to us) based on only the vortex structure and the wind speed. The goal was to cover a wide range of wind speeds and vortex structures so that the data can be used for calibrating a large variety of experimentally/numerically simulated vortices. That being said, five tornado events were chosen for this study: Spencer, SD 1998 (F4), Stockton, KS 2005 (F1), Clairemont, TX 2005 (F0), Happy, TX 2007 (EF0) and Goshen County, WY 2009 (EF2) tornadoes. The GBVTD method was used to analyze single-Doppler radar data from these five tornado events.

Data acquired through a complete radar scan of a tornado from regions beginning very close to the ground and ending hundreds of meters aloft is termed as a "volumetric sample" or "volume" in short. Out of the five tornadoes mentioned above, a total of nine volumes of radar data were investigated in this study to retrieve three-dimensional structure of the parent vortex. The number of radar sweeps in a volume varied between 4 and 14 with the finest and coarsest elevation angle increments of 0.3° and 6°, respectively. The minimum observation height varied as a function of the intervening terrain and/or the distance from the radar to the center of rotation. Volumes were selected to cover wind speeds associated with EF0- to EF3-rated tornadoes based on the maximum GBVTD-retrieved velocity.

The GBVTD analysis consists of four steps: filtering the raw radar data, transforming the data into a Cartesian grid, identifying the center of the vortex and retrieving tangential and radial velocity components through the algorithm detailed in [7]. In the following paragraphs, these four steps are briefly explained. A more detailed discussion of the process can be found in [49,50,7].

Volumes of radar data were first filtered subjectively using the SOLO II software [51] to remove noise and any spurious data resulted from ground clutter and signal blockage near the surface. Then, the data were mapped to a Cartesian grid (Δx, Δy, Δz) using a bilinear interpolation scheme [49]. Vortex center coordinates were identified based on the findings of Wood and Brown [50], which suggested that, given an axisymmetric flow field, the center of the tropical cyclone is located on a circle that passes through the radar and Doppler velocity maxima. Therefore, the circulation centers were identified for every volume and at each elevation angle of the radar in accordance with this approach while taking into account the asymmetry inherited in the flow field of tornado vortices. The tornado circulation center at each elevation was then shifted to vertically align the centers in order to account for the time evolution in the wind field.

In the GBVTD method, velocity components normal to the radar beam are retrieved under the assumption that the tornado is circular. Therefore, the GBVTD analysis is applied to a ring with the circulation center of the vortex located at the center of this ring. The Doppler velocity (V_D) is expressed as a function of tangential (V_{tan}), radial (V_{rad}), translational (V_{trans}) and axial (V_{ax}) velocities of the atmospheric vortex as well as the terminal velocity of hydrometeors and debris (v_t):

$$V_D = V_{trans}\cos(\gamma - \theta_M)\cos\varphi - V_{tan}\sin\psi\cos\varphi + V_{rad}\cos\psi\cos\varphi + (V_{ax} - v_t)\sin\varphi \quad (1)$$

where φ is the elevation angle of the radar beam, θ_M is the direction of the mean wind flow and, ψ and γ are results of the observational geometry as shown in Fig. 1 of Lee et al. [7]. Contributions from the terminal velocity of hydrometeors and debris and the axial velocity are neglected as only the axisymmetric velocity fields are investigated. The horizontal velocities (tangential and radial components) consist of axisymmetric and asymmetric components. In this analysis, it is assumed that the flow field is dominated by strong axisymmetric tangential velocities. After simplifying the equations and implementing the complex geometrical relationship between an atmospheric vortex and the DOW, a system of equations relating Doppler velocities to the tangential and radial velocities are solved to retrieve the horizontal velocity field (i.e. azimuthally averaged tangential and radial velocities). Then, the axial velocity at each grid point is determined through upward integration of the continuity equation with a no slip boundary condition at the ground. Mathematical representation of this method and full assumptions are explained in detail by Lee et al. [7].

Fig. 3 shows a contour map of Doppler velocities for the Happy, TX 2007 tornado (hereafter Hp tornado) at 0203:20 UTC (Coordinated Universal Time). The wind field of this tornado was reconstructed for a volume from 0203:20 UTC to 0204:09 UTC (hereafter v2). This volume consisted of 13 radar sweeps with elevation angle increments ranging from 0.3° to 2°.

Fig. 4a depicts the vertical (axial-radial) velocity vector map superimposed on the contour map of tangential velocities for Hp v2 tornado extracted using the GBVTD method. It is observed that the tangential velocity approaches its maximum of 38 m/s at regions close to the ground (approximately 40 m Above Ground Level (AGL)) with corresponding core radius (r_c) of 160 m. The central downdraft aloft is weakening as it reaches the ground and the overall vertical flow pattern suggests that the vortex breakdown "bubble" formed aloft has just touched the ground [20].

As previously addressed, the radial and, consequently, the axial velocities obtained from the GBVTD analysis can be affected by the centrifuging of hydrometeors and debris. Using a linear analytical

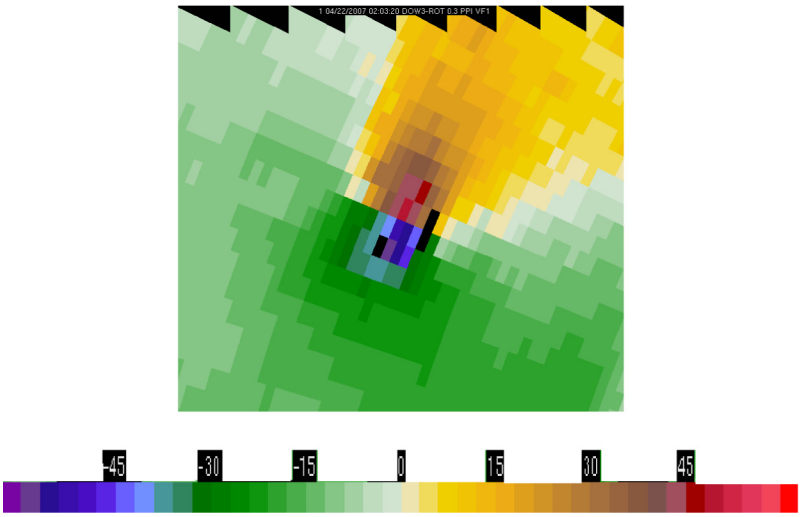

Fig. 3. Plan Position Indicator (PPI) map of Doppler velocity (m/s) for the Happy, TX 2007 tornado at 0203:20 UTC (Hp v2) and at 0.3° radar elevation angle.

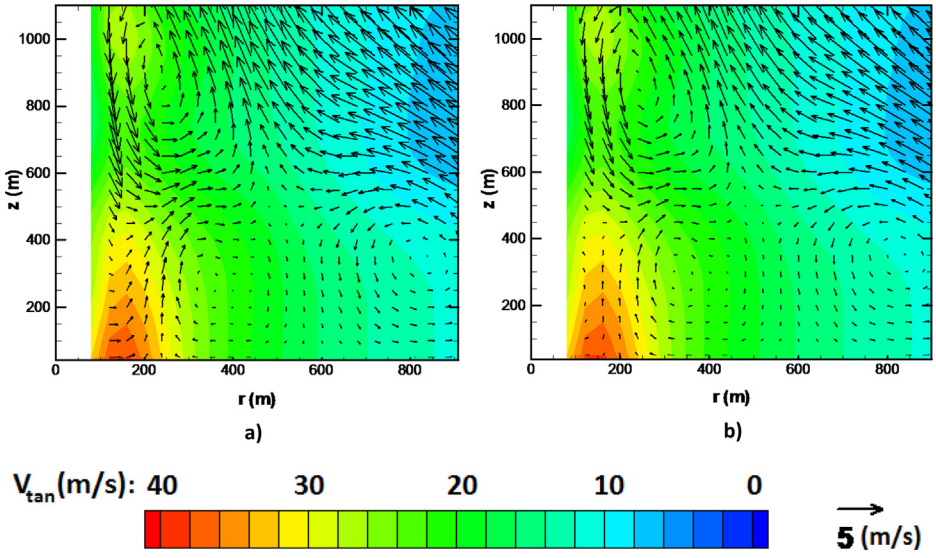

Fig. 4. GBVTD retrieved structure of the Hp v2 at 0203:20 UTC, vertical (axial-radial components) velocity vectors superimposed on tangential velocity (contours). (a) Without and (b) with correction for centrifuging effect of small raindrops.

Table 1
Summary of GBVTD analysis results. Volumes are sorted in an increasing order of tangential velocity and the vortex structure determined for each volume is presented.

	Clairemont, volume1 (Clr v1)	Happy, volume2 (Hp v2)	Happy, volume1 (Hp v1)	Goshen Co, volume1 (GC v1)	Goshen Co, volume2 (GC v2)	Goshen Co, volume3 (GC v3)	Stockton, volume1 (Stc v1)	Spencer, Volume1 (Sp v1)	Spencer, Volume2 (Sp v2)
EF-/F-Scale (based on damage survey)	F0	EF0	EF0	EF2	EF2	EF2	F1	F4	F4
Time interval (UTC)	2328:32-2328:44	0203:20-0204:09	0159:53-0200:57	2216:06-2216:45	2218:07-2218:42	2218:50-2219:39	2240:26-2240:38	0135:20-0135:52	0140:02-0140:41
Elevation angles (°)	0.3, 1, 1.7, 2.4	0.3, 0.6, 1, 1.5, 2, 2.5, 3, 4, 5, 6, 7.1, 9, 11	0.5, 1, 2, 3, 4, 5, 6	1, 2, 3, 4, 5, 6	0.5, 1, 2, 8, 10, 12, 14, 16	0.3, 1, 1.7, 2.4	2.5, 3.4, 5.4, 7.6, 10.2, 13.1, 16.3, 20.6	0.6, 1, 1.5, 2.5, 3.4, 5.5, 7.4, 10.5, 13.3, 16.5	
$\Delta x = \Delta y$ (m)	18	50	40	25	25	25	20	16	16
Δz (m)	40	50	50	42	40	41	40	40	40
z_{min} (m)	25	38	71	47	75	30	43	51	51
V_{trans} (m/s)	1.2	19.4	19.4	9.49	9.49	9.49	10.95	15	15
$V_{tan,max}$ (m/s)	36.3	37.9	39	42.2	42	42.9	50.7	60.2	64.1
$r_{c,max}$ (m)	96	160	160	150	150	100	220	192	208
z_{max} (m)	200	50	250	47	160	41	43	51	51
EF-scale (based on $V_{tan,max}$)	High-end EF0	High-end EF0	Low-end EF1	Low-end EF1	Low-end EF1	Mid-range EF1	Low-end EF2	High-end EF2	Low-end EF3
Vertical structure	VBD aloft	Touch-down	Single-celled	Two-celled	Transition stage	Two-celled	Single-celled	Two-celled	Two-celled

model for a translating tropical cyclone, Kepert [52] showed that in a rotating boundary layer there must exist a radial inflow at and around the radius of overall maximum tangential velocity. However, the net pressure force that accelerates the flow inward is weak compared to the centrifugal force that moves dense particles outward relative to the air and, as a result, the expected low-level inflow is not observed in retrieved data. To account for the centrifuging effect of hydrometeors and debris, the radial velocity components were modified ($V_{rad,mod}$) using the following equation proposed by Nolan [47]

$$V_{rad,mod} = V_{rad} + V_{rad,bias} = V_{rad} + C_{max}\left[\frac{V_{tan}^2/r}{\max\{V_{tan}^2/r\}}\right] \quad (2)$$

where $V_{rad,bias}$ is the positive bias in the radial velocity values due to the centrifuging of particles and C_{max} is the terminal fall speed of dominant particles in the flow (e.g. raindrops, hailstones, debris) as provided by Dowell et al. [48]. Information regarding scatterers' size and type can be provided by the observers at the site of a tornado or can be estimated based on the underlying surface of the site and whether the tornado has passed through structures or not. Given the limited availability of such information for the tornadoes that were analyzed here, the vertical wind field of these events is only corrected for small raindrops (0.5 mm in diameter). For more information on centrifuging effect of hydrometeors and debris on radar-retrieved data refer to Nolan [47] and Dowell et al. [48].

Fig. 4b displays the flow field of the Hp v2 corrected for centrifuging influence of small raindrops. When compared to Fig. 4a, it is seen that the divergence at lower elevations has decreased while the updraft has slightly intensified. Note that the research on the debris centrifuging effect is at its early stages and is not yet mature. For instance, currently most algorithms, including the one employed in this work, assume that the centrifuging effect is evenly distributed over the whole flow field. However, an important consideration is that large debris will be confined to lower parts of the tornado. Therefore, when correcting for the centrifuging effects of large scatterers, it is important to have an estimate of the affected depth of the flow.

Following the approach detailed above for the Hp v2 volume, the remaining eight tornado volumes were analyzed. A summary of the main information regarding each volume of data analyzed here as well as the parameters used in and extracted from the GBVTD method are provided in Table 1. The damage-based F- and EF-Scales for each tornado event were determined using the Storm Events Database [1]. The time interval and the radar elevation angle associated with each volume, the grid spacing and the minimum height (z_{min}) scanned by the radar are also presented in Table 1. The values of grid spacing are dictated by the radar resolution near the center of the tornado. Choosing a larger value for the grid size results in an excessive smoothing of the data, while selecting a much smaller value adds noise to the calculation [53,54].

The translational speed of the tornado was approximated based on the distance that the tornado had traveled over radar observation time. The overall maximum tangential velocity ($V_{tan,\max}$) obtained for each volume from the GBVTD analysis and the corresponding radius ($r_{c,\max}$) and height (z_{max}) are also provided in Table 1. Note that the values reported in Table 1 and used to plot the results are all grid values and not the measured values. Also, since the surface layer in tornado flows is under debate and more evidence is needed to clarify the structure of that layer, any extrapolation of the data to a grid point below z_{min} is avoided.

Sensitivity of the GBVTD analysis to the vortex center location as well as the grid spacing were examined. Errors smaller than 20% of the radius of the maximum tangential velocity (r_c) in the center location identification and changes in the grid size by ±8%

of the largest radar resolution at the tornado center resulted in negligible changes in the tangential velocity profiles and the flow structure.

4. Results and discussion

Results are divided into two sections: Section 4.1 presents the three-dimensional velocity field obtained from the GBVTD analysis and discusses the *tornado events*. Section 4.2 analyzes the entire preliminary database, which consists of nine *volumes*, in an attempt to correlate each of the volumes to their fluid mechanics characteristics.

4.1. Individual event flow field analysis

Fig. 5 displays the GBVTD-analyzed structure of each volume of tornado data. In these figures, the vertical velocity vector map is superimposed on the contour map of the tangential velocity. Results are corrected for the effect of centrifuging of small raindrops on the flow structure.

Given the primary objective of this work, initiating a preliminary database of tornado full-scale flow data for engineering applications, identifying the vertical structure of each volume of tornado data is essential. In order to determine the vortex structure, the vertical velocity vector map of each volume analyzed herein is qualitatively compared with Fig. 2. As discussed in Section 2, variation of the swirl ratio results in various tornado flow structures [19,23] among which the most important are the vortex breakdown, vortex breakdown reaching the ground, two-celled vortex and multiple vortices.

The very weak Clairemont, TX tornado (hereafter Clr tornado) formed at 2305 UTC on 12 June 2005. This tornado was scanned by the DOW3 radar using four elevation angles ranging from 0.3° to 2.4°, resulting in measurement data at as low as 25 m AGL. The vertical velocity vector map of this tornado at 2328:32 UTC (hereafter v1), shown in Fig. 5a, suggests a downdraft that weakens near the surface. Also, the maximum tangential velocity is observed away from the surface. This configuration matches Fig. 2c of the work by Davies-Jones et al. [19] well and corresponds to the stage of tornado vortex evolution just before the touch-down.

Another weak tornado was intercepted by DOW3 the evening of 21 April 2007 near the town of Happy, TX (hereafter Hp tornado). This tornado was scanned from 0158:16 UTC to 0207:22 UTC and for various elevation angles ranging from 0.3° to 13.1°. Fig. 5b illustrates a single-celled structure (compare with Fig. 2b) with an updraft close to the center of the vortex at 0159:53 UTC (hereafter v1). A very weak outflow is detected at 400 m AGL and higher elevations. Applying the correction for centrifuging of small rain drops increased the maximum inflow by 34% and intensified the updraft at the centerline. Approximately 3.5 min later, at 0203:20 UTC (hereafter v2), a downdraft of 12 m/s is observed at very high elevations (~900 m AGL) while the updraft is shifted away from the centerline (Fig. 5c). Also, the overall maximum tangential velocities are now moved towards the surface and the vertical structure of the vortex is comparable with Fig. 2d. It is debatable if this configuration represents the stage immediately before or after the touch-down of the vortex breakdown (VBD) bubble as the core region is not fully resolved.

The 5 June 2009 long-lasting EF2-rated tornado of Goshen County (LaGrange), WY (hereafter GC tornado) was intercepted by DOWs during the VORTEX2 project [55–58]. The GC tornado event has been thoroughly investigated over its lifetime through photogrammetric analysis combined with single- and dual-Doppler radar analysis. This long lasting tornado started at 2152 UTC and ended at 2231 UTC. In a study by Wakimoto et al. [44], the three-dimensional structure of this tornado was extracted using the GBVTD method for two different volumes; 2216:08-2216:45 UTC (hereafter v1) and 2218:07-2218:42 UTC (hereafter v2). Three volumes of the GC tornado, including the two that have been previously analyzed by Wakimoto et al. [44], were selected for analysis in the current study. This provides the opportunity to examine the robustness of the retrieval analysis.

The flow field approximated for GC v1 is shown in Fig. 5d. The core region of the flow, which is about 300 m wide, and the surrounding area are dominated by a downdraft. A very weak updraft is observed away from the core at $r = 350$ m. The overall reconstructed flow field is in good agreement with the one reported by Wakimoto et al. [44]. Since the flow field is dominated by a downdraft, it is difficult to characterize the vertical structure of the flow. However, axial downdrafts exceeding 17 m/s very close to the centerline together with weak updrafts that are located at the periphery of the funnel as shown by Wakimoto et al. [44], suggest a two-celled vortex pattern. After 2 min in the GC v2 (see Fig. 5e), the velocity field is still dominated by downdrafts and outflows while a local peak in the value of the overall maximum tangential velocity is apparent at 160 m AGL. The lowest radar data available for this volume is at 75 m AGL, which means that the inflow layer is likely not resolved in this case. The retrieved flow field of the GC v2 is well matched with the one presented by Wakimoto et al. [44]. When compared to GC v1, the downdraft has weakened slightly while there is no evidence of updraft at the periphery of the funnel. These observations combined with the fact that the overall maximum tangential velocity is captured at relatively high elevations suggest that the tornado vortex is transitioning from a supercritical condition to a subcritical stage. Fig. 5f depicts the GBVTD-extracted velocity field of the third volume of the GC tornado scanned at 2218:50 UTC (hereafter v3). The core radius shrinks by 30% when compared with GC v1 and GC v2 and the overall maximum tangential velocity shifts back towards the ground. Relatively strong downdrafts confined to the core along with updrafts right outside of the vortex core are consistent with the vertical structure of a two-celled vortex (see Fig. 2e). A persistent downdraft in all three volumes of the GC tornado confirms that the tornado is at the dissipation stage. Further investigations of the axial profile of the tangential velocity for GC v1-v3, presented later in this study, may provide more insights into the vertical field of the vortex.

DOW3 intercepted a tornado near Stockton, KS on 9 June 2005 (hereafter Stc tornado) at 2157 UTC. Although this tornado was rated F1, wind speeds as high as 50 m/s were measured by DOW3 in this event. The Stc tornado was briefly (from 2239:11 UTC to 2240:38 UTC) scanned by DOW3 and the GBVTD-retrieved velocity field of one volume (hereafter v1) of data is presented in Fig. 5g. The vortex core is approximately 440 m wide with the lowest height scanned by the radar being 43 m AGL. The flow is dominated by inflow and consequently an updraft of approximately 21 m/s in the core region which is representative of a single-celled vortex structure.

On 31 May 1998 an F4 rated tornado impacted the town of Spencer, SD killed 6 people and left behind $17 million worth of property damage. DOW3 collected data from this tornado (hereafter Sp tornado) at 0100 UTC for approximately 45 min. Herein, two volumes of Sp tornado data, at 0135:20 UTC (hereafter v1) and 0140:02 UTC (hereafter v2) were investigated. The Sp tornado vortex core reached the city at 0138:08 UTC and exited at 0139:30 UTC.

The vertical structure of the flow in Fig. 5h for Sp v1 indicates two-celled vortex (compare with Fig. 2e) characteristics with a very strong downdraft of 62 m/s close to the center at 720 m AGL. As noted by Fiedler and Rotunno [59] such a strong downdraft is a characteristic of two-celled tornadoes. The overall maximum

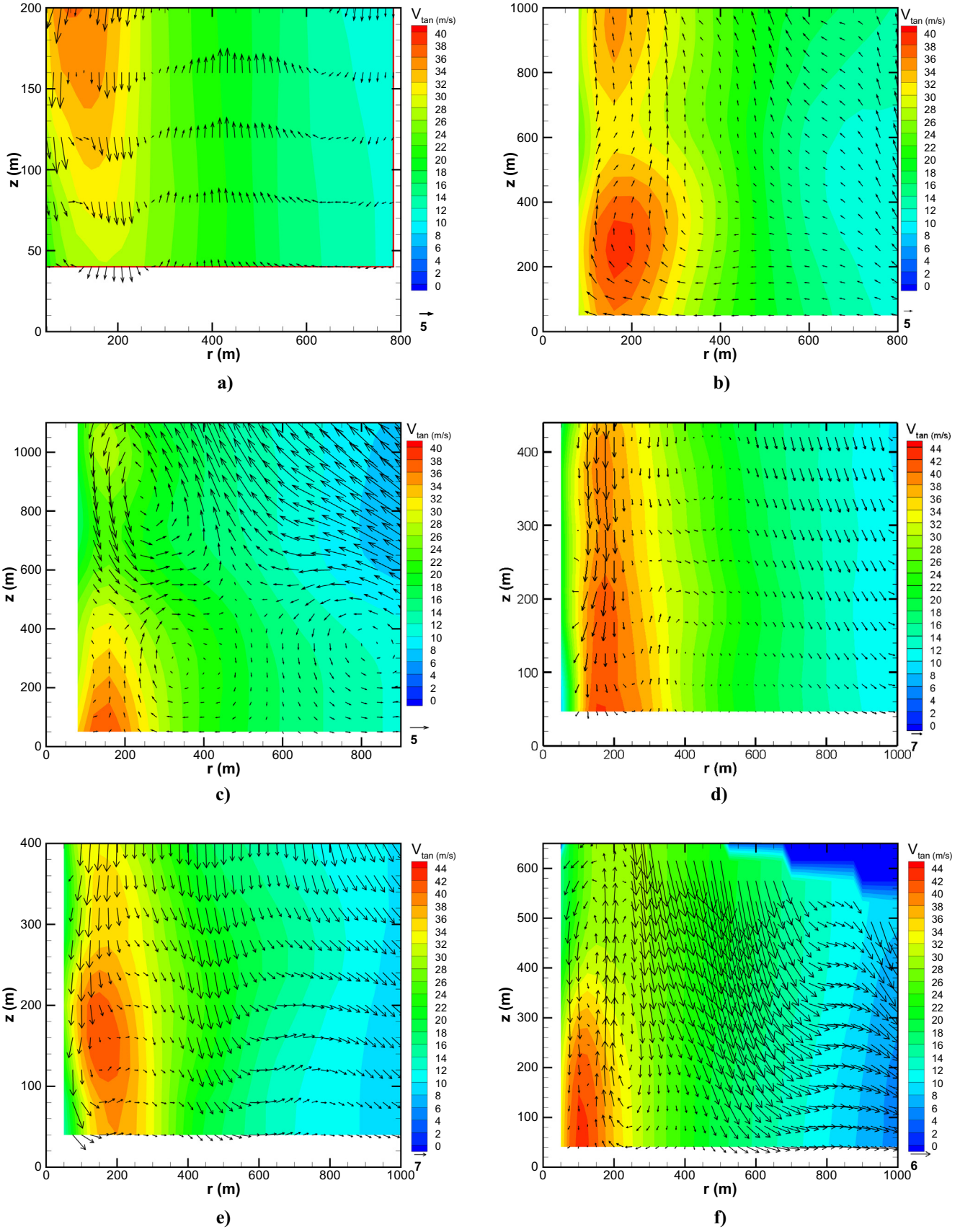

Fig. 5. Vertical (axial-radial components) velocity vectors superimposed on tangential velocity contours for (a) Clr v1 at 2328:32 UTC, (b) Hp v1 at 0159:53 UTC, (c) Hp v2 at 0203:20 UTC, (d) GC v1 at 2216:08 UTC, (e) GC v2 at 2218:07 UTC, (f) GC v3 at 2218:50 UTC, (g) Stc v1 at 2240:26 UTC, (h) Sp v1 at 0135:20 UTC and (i) Sp v2 at 0140:02 UTC.

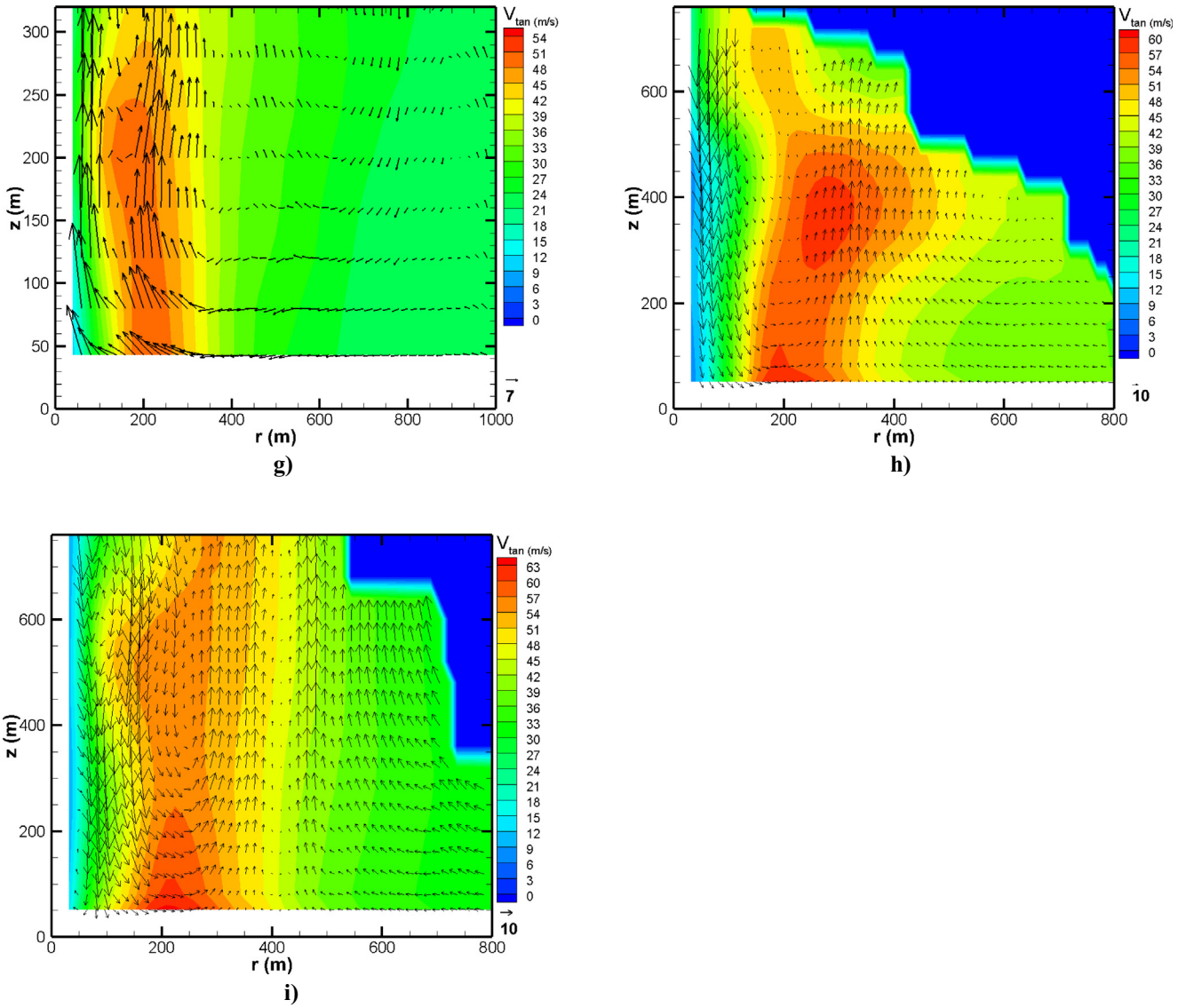

Fig. 5 (*continued*)

tangential velocity of 60.2 m/s is obtained at 51 m AGL and at a radius of 192 m. Radar measurements are available for this volume at 51 m AGL or higher. Fig. 5h illustrates a local peak in the tangential velocity values at higher elevations (~350 m AGL). As discussed by Kosiba and Wurman [37], this could be a retrieval analysis error due to the temporal resolution of the radar. In other words, the tornado intensification between successive scans is represented as a local peak in the tangential velocities aloft.

The wind field of the Sp v2 is displayed in Fig. 5i. Similar to the Sp v1, a wide rotation is accompanied by a strong downdraft close to the centerline. The vertical wind map is in very good agreement with Fig. 2e of the work by Davies-Jones et al. [19] which suggests a two-celled vortex flow. Maximum tangential velocities are observed close to the surface and the updraft is shifted away from the centerline. The overall maximum tangential velocity of 64.1 m/s at a radius of 208 m is estimated for this volume.

4.2. Investigation of the preliminary database

In this section, the focus is on analyzing the preliminary database of tornado volumes to investigate potential correlation between the swirl ratio and structure of field vortices and their associated EF-Scale. Assessing the intensity of a tornado based on damage surveys is highly subjective to accessibility, damage indicators in the region and quality of structures and as a result, may not be representative of true tornado intensity. For instance, DOW measured data suggest that the Hp tornado was stronger than EF0. Yet it travelled through an open country terrain and, as a result due to the lack of indicators, it is most likely underrated. Therefore, using the velocity range associated with each category of the EF-Scale to rate tornado volumes is deemed more practical, particularly for engineering applications. Subsequently, the volumes of data analyzed in Section 4.1 are presented in Table 1 in an ascending order of EF-Scale based on the overall maximum tangential velocity value. In addition, since there is a range of velocities associated with each EF-Scale, the tornado volumes in Table 1 are categorized as low-end, mid-range and high-end. The vertical structure of the vortex for each volume, as determined in Section 4.1 through qualitative comparison of GBVTD-retrieved vortex flow field with Fig. 2, is also reported in Table 1. An interesting observation is that once the volumes are ranked based on the maximum tangential velocity (rather than damage survey results), the

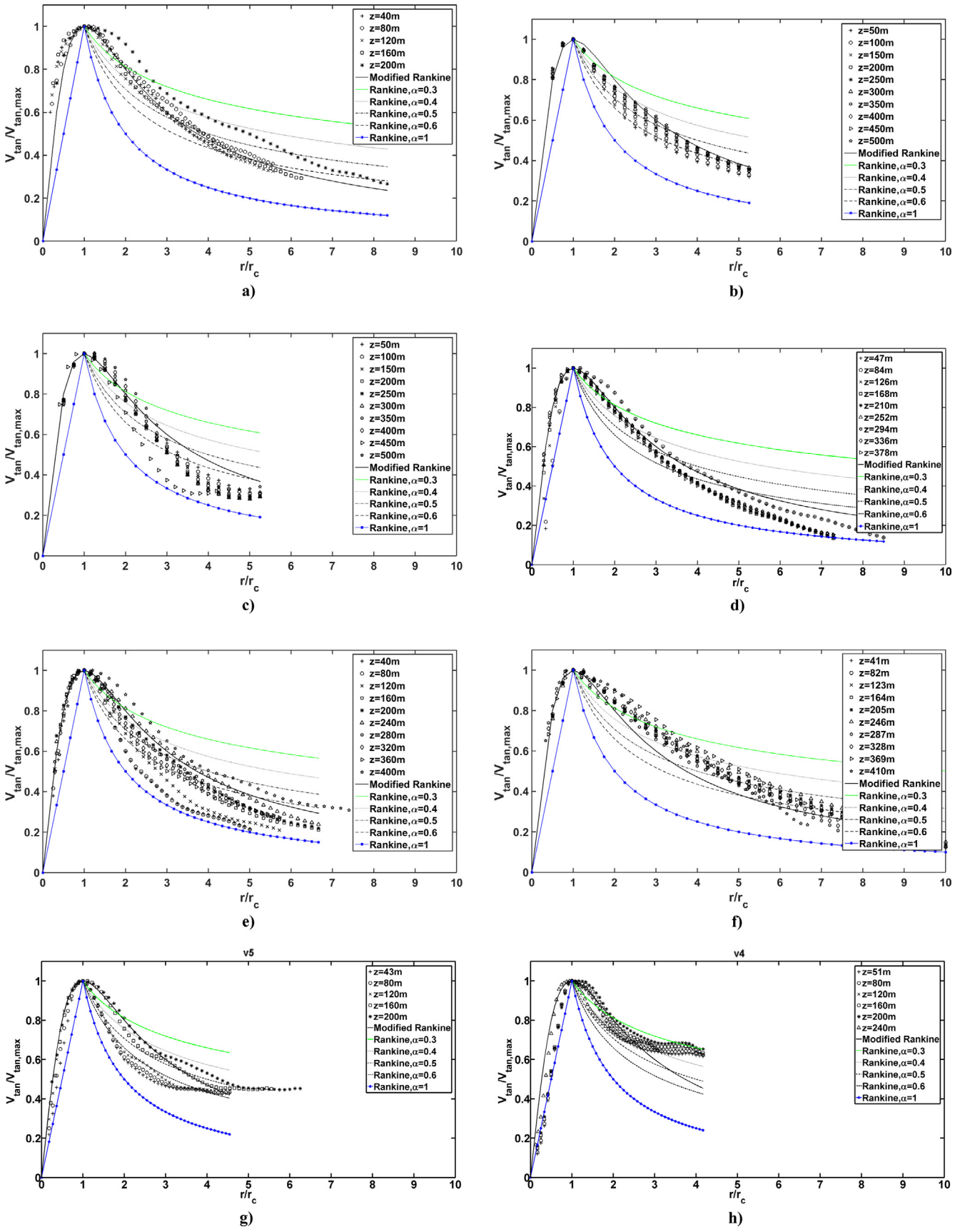

Fig. 6. Radial profiles of tangential velocity at different heights compared a Modified Rankine Vortex model and Rankine Combined Vortex model for (a) Clr v1 (EF0), (b) Hp v2 (EF0), (c) Hp v1 (EF1), (d) GC v1 (EF1), (e) GC v2 (EF1), (f) GC v3 (EF1), (g) Stc v1 (EF2), (h) Sp v1 (EF2) and (i) Sp v2 (EF3).

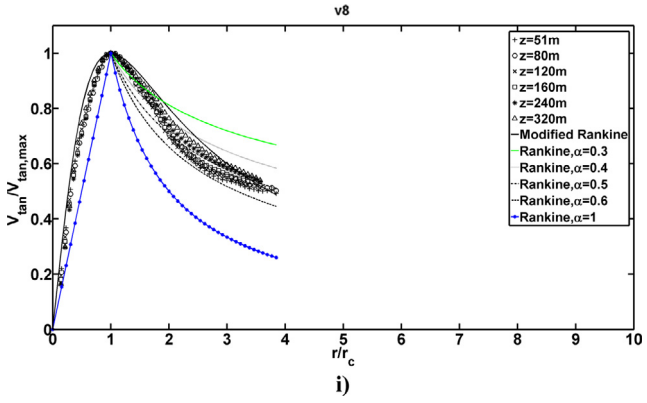

Fig. 6 (*continued*)

full-scale tornado vortex structure variation with the maximum tangential velocity matches the vortex structure evolution as a function of swirl ratio as suggested by Davies-Jones et al. [19] and other experimental works [10,13]. Note that hereafter, all results are presented in an increasing order of EF-Scale and an EF-Scale refers to the one based on Doppler-measured velocity rather than damage-estimated velocity.

In addition to the data in Table 1, the velocity profiles of the investigated tornado volumes can be used as a benchmark for experimental and numerical simulations of tornado-like vortices. It is known that the radial, and consequently the axial, velocities are sensitive to the correction for centrifuging effects. In addition, detailed information about scatterer size and type were not available for most of the tornado events studied here. As a result, only tangential velocity profiles, which are less impacted by scatter type, are presented. The tangential velocity variation with radius is plotted in Fig. 6 for all volumes of data and at various heights. Velocities and radii are normalized using the maximum tangential velocity and the core radius corresponding to each height, respectively. Results are compared with a Modified Rankine Vortex model suggested by Houston and Powell [60] in which the tangential velocity is estimated using $V_{tan} = 2r_{c,max}V_{tan,max}\, r/(r_{c,max}^2 + r^2)$. A Rankine Combined Vortex model (with different decay factors, α) as proposed by Depperman [61] is also used for comparison with full-scale data. In this model the vortex tangential velocity is defined as $V_{tan} = V_{tan,max}\, r/r_{c,max}$ for the core region and $V_{tan} = V_{tan,max}\,(r_{c,max}/r)^{\alpha}$ for the outer core region. The overall maximum tangential velocity ($V_{tan,max}$) of each volume and the corresponding radius ($r_{c,max}$) were used to calculate the tangential velocity in these models. Overall, the Modified Rankine Vortex is in better agreement with the field measurements. Also, decay factors of 0.4–0.6 result in better match with the full-scale data which is consistent with the findings of previous studies [35–37]. No correlation between the decay factor and the volume intensity is observed. Discrepancies are spotted at lower heights and at the outer core region of the vortex between the Modified Rankine Vortex and the Doppler-measured data. As explained by Snow [62], idealized profiles such as Rankine vortex are most applicable above the surface layer, where radial velocities are relatively weak. The Clr v1 and Hp v1 are exceptions as the best agreements are achieved at lower elevations. This may be explained by their supercritical core at lower elevations, which means less surface interactions [10,13]. In addition, discrepancies between the retrieved tangential velocities of Sp v1 and the estimated velocities using the Modified Rankine Vortex model at radial distances far from the vortex core may be due to the presence of subvortices in the full-scale data.

Experimental [63] and numerical [64,65] simulations have shown that the axial profile of the maximum tangential velocity

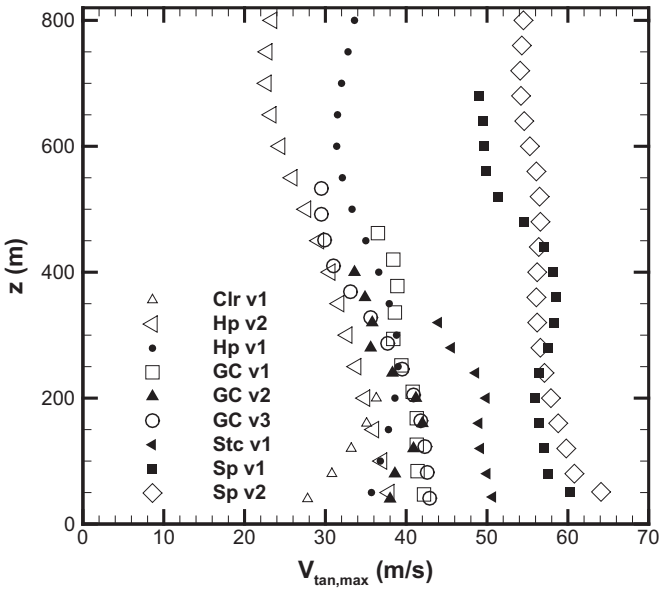

Fig. 7. Variation of the maximum tangential velocity with height for various volumes of radar data.

in tornado-like vortices is distinctly different from the typical straight winds profiles. Such velocity profiles in tornado flows are rather flat in the near-surface region or present a local maximum very close to the surface. This characteristic of tornadic flow fields is thought to be associated with the different loading and collapse modes of structures in tornado events compared to straight winds. In order to further assess this aspect for real tornadoes, the axial profiles of the maximum tangential velocity are drawn in Fig. 7 for all volumes of data. Except for the Clr v1, Hp v1 and GC v2, the maximum tangential velocity increases as moving towards the ground. However, there is no evidence of a local maximum of tangential velocities close to the surface. In a recent study performed by Kosiba and Wurman [41], the near surface flow of the EF2 rated Russell, KS tornado of May 2012 was retrieved and the maximum tangential velocities were located at the lowest heights ($z < 10$ m AGL). Therefore, it may be that, if present, the maximum in the current data is at elevations that are not resolved by the radar measurements, particularly for weaker tornadoes. On the other hand, Fig. 7 demonstrates minimal variations in the tangential velocities at the lowest data points for Hp v2, GC v1, GC v3 and Stc v1. A similar trend was reported by Kosiba and Wurman [41]. They observed a gradual decrease of about 10% in the Doppler velocities from 10 m to 40 m AGL. Therefore, one may conclude that the axial profiles of the tangential velocity reported here correspond to the regions right above the inflow or the boundary layer of the tornado vortex.

Fig. 7 suggests a different trend for axial profiles of the maximum tangential velocity for Clr v1, Hp v1 and GC v2, when compared to trends observed for other volumes. The overall maximum tangential velocity for Clr v1, Hp v1 and GC v2 is captured at relatively high elevations ($z > 160$ m AGL). This trend implies that the vortex is at transition, from a supercritical stage to a subcritical stage, which is consistent with the retrieved vertical structure of Clr v1 and GC v2.

As discussed before, experimentally and numerically simulated tornado vortices are governed by the swirl ratio. However, determining the swirl ratio of a field tornado is very challenging as S is defined based on the boundaries of physical simulators and these boundaries are not easily distinguishable for real tornadoes. Calculating the swirl ratio of field tornadoes has been attempted by

Lee and Wurman [35] and Kosiba and Wurman [37] for the Mulhall (hereafter Ml tornado) and the Sp tornadoes, respectively. They estimated swirl ratios of 2–6 for the Ml tornado and 1–7 for the Sp tornado. In both studies, it is stated that this range of swirl ratios is consistent with the multiple vortex radar signatures observed in these events. However, Kosiba and Wurman acknowledged that due to the underrepresentation of the radial inflow in radar measurements, the swirl ratio values might have been overestimated. The swirl ratio in both aforementioned studies is calculated using $S = (1/2a)V_{tan}/V_{ax}$ in which V_{tan} and V_{ax} are both determined at the updraft radius.

Alternatively, the swirl ratio can be expressed using the maximum circulation (Γ_∞) in the flow and the volumetric flow rate (Q') through the updraft region [66]: $S = r_0\Gamma_\infty/2Q'$. In this equation, Γ_∞ is calculated using the overall maximum tangential velocity and the corresponding radius. Computing the swirl ratio of the field data using the circulation may result in more accurate values as it reduces the error associated with subjectively choosing the representative values. Herein, the swirl ratio associated with each volume was determined by calculating the average flow rate through the updraft and the maximum circulation. As an attempt, the updraft region is identified at the highest available radar scan and is defined as an area for which the axial component of the velocity is larger than the radial component. The estimated swirl ratios and the values chosen for calculating S are reported in Table 2. Since the flow was dominated by downdraft for the GC volumes, it was not possible to estimate the updraft region and therefore, swirl ratio is not reported for these volumes. It is seen that swirl ratio values vary between 1 and 5 for the volumes studied here.

It was expected to obtain the maximum swirl ratios for Sp v1 and Sp v2 as they showed a two-celled vortex structure with large tangential velocities. Yet, the maximum swirl ratios were computed for Clr v1 and Stc v1. Further investigations showed that the last radar scan in aforementioned volumes was limited to 200 m and 320 m AGL, respectively. This results in an underestimation of the flow rate aloft and therefore, high values of the swirl ratio. The updraft region definition is the main contributing factor to the underestimation of the flow rate for cases with limited radar-scanned heights such as Clr v1 and Stc v1. The flow rate used in the swirl ratio equation is defined as the volumetric flow rate through the *updraft region*. So, once the updraft radius is known, the flow rate can be calculated by multiplying the axial velocity by the updraft area. Since the term updraft region comes from tornado simulators, it is not easily distinguishable in field tornadoes. As mentioned before, in this study it is assumed that the updraft region is located at the highest available radar scan and is defined as an area for which the axial component of the velocity is larger than the radial component. Let's consider the case that radar data is only available up to $z = z_1$ (see Fig. 8). By definition, the updraft radius (where the axial component of the velocity is larger than the radial component) for this case equals to $r_{0,1}$. Now let's consider that for the same tornado vortex, radar data is available up to $z = z_2$. where, $z_2 > z_1$. In this case, by definition, the updraft radius equals to $r_{0,2}$. where, $r_{0,2} > r_{0,1}$. Therefore, the height at which the updraft radius is selected at can affect the flow rate calculations. In another word, the lower the height at which the updraft radius is determined at, the lower the flow rate value and therefore, the higher the value of the swirl ratio.

Table 2
Estimated swirl ratio and the corresponding chosen parameters for each volume.

volume	$r_{c,\max}$ (m)	$V_{tan,\max}$ (m/s)	r_0 (m)	Q' (m^3/s)	S
Clr v1	96	36.3	608	1.4×10^6	4.5
Hp v2	160	37.9	720	13.5×10^6	1.01
Hp v1	160	39	600	11.2×10^6	1.04
Stc v1	220	50.7	600	4×10^6	5.13
Sp v1	192	60.2	512	8.2×10^6	2.25
Sp v2	208	64.1	608	8.2×10^6	3.09

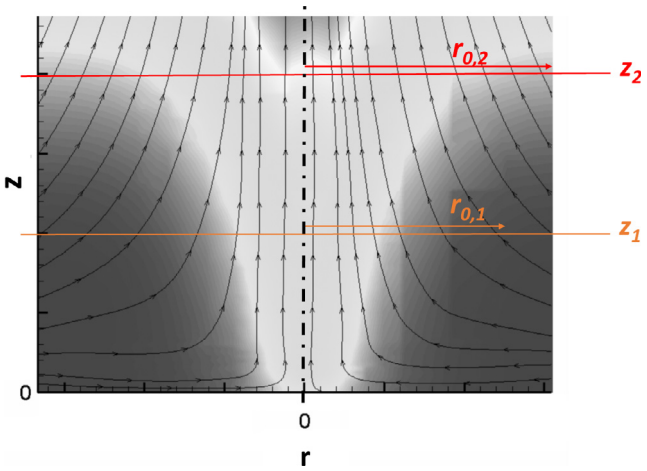

Fig. 8. Dependency of the flow rate value on the maximum height scanned by radar.

Excluding Clr v1 and Stc v1 from the discussion, results obtained in Table 2 suggest dependency of vortex structure on the swirl ratio as suggested by laboratory investigations [10,19,66]. By comparing the estimated swirl ratios with the vertical structure of the vortex for each volume of data (reported in Table 1), one can conclude that as the swirl ratio increases the vortex structure changes from a single-celled vortex with VBD aloft to the touch-down stage and eventually to two-celled and multiple vortices.

Overall, discrepancies between the swirl ratios calculated using the full-scale data and the laboratory measurements are highly expected mostly due to the uncertainties in identifying the updraft region and in the retrieved inflow regions. However, when compared to previous attempts [35,37] that calculated the swirl ratio of field tornadoes, the alternative approach implemented in the current study (swirl ratio as a function of maximum circulation and the volumetric flow rate) resulted, as expected, in swirl ratios that are closer to the laboratory reported S values [67,68].

5. Conclusions

In a first attempt to create and analyze a preliminary database of full-scale tornado wind fields, nine volumes of single-Doppler radar data were investigated. These volumes were selected to cover a wide range of wind speeds and vortex structures and correspond to EF-Scales between EF0 and EF3, based on the maximum tangential velocity. The recently established mathematical method, namely GBVTD, was implemented to reconstruct the three-dimensional velocity field of these tornado volumes. Identification of field tornado vortex structure, i.e. single-celled vortex, vortex breakdown bubble formation aloft, vortex breakdown bubble touch-down and two-celled vortex, as well as the relationship between these flow field features and swirl ratio and potentially to EF-Scale is of particular interest for laboratory and numerical simulations of tornado-like vortices. Tangential velocity contour maps combined with the vertical velocity vectors, all retrieved by the GBVTD, were used to determine the vortex structure. Among the nine volumes of data studied herein, Hp v1 and Stc v1 showed single-celled characteristics, vortex breakdown bubble was evident in Clr v1, Hp v2 was at the touch-down stage and, GC v1, GC v3, Sp

v1 and Sp v2 showed two-celled vortex characteristics. Maximum velocities deduced from the full-scale data ranged between 36 m/s and 64 m/s. The radial profiles of the tangential velocity were compared with two analytical models and a good agreement was found between the full-scale measurements and the Modified Rankine Vortex model, particularly at higher altitudes. In addition, it was observed that for the range of heights analyzed the vertical profiles of maximum tangential velocities are very different compared to typical atmospheric boundary layer profiles. In addition, the swirl ratio of full-scale data was computed, for the first time, using the flow rate through the updraft and the maximum circulation in the flow.

This preliminary database along with the calculated swirl ratios provide an insight into the flow field of tornadoes for a limited but good variety of vortex structures and intensities. Following the approach developed here, this preliminary database can be extended and can be used to provide much needed information in order to properly scale and simulate tornado-like vortices both physically and numerically. This in change can provide the basis of experimentally investigating the wind loading and structural impacts of tornadoes on buildings and structures.

Acknowledgment

The authors acknowledge the following funding supports: NSERC#R2811A03 and NSF-AGS#1211132, NSF-AGS#1361237, NSF-AGS#1447268. Also, special thanks to Paul Robinson for assisting with data analysis and Abby Arnold for proofreading the manuscript.

References

[1] Storm Events Database. <www.ncdc.noaa.gov/stormevents/>, Aug 2013 n.d.
[2] Smith A, Lott N, Houston T, Shein K, Crouch J, Enloe J. U.S. billion-dollar weather & climate disasters 1980–2016. NOAA National Centers for Environmental Information; 2016.
[3] Kuligowski ED, Lombardo FT, Phan LT, Levitan ML, Jorgensen DP. Final Report, National Institute of Standards and Technology (NIST) Technical Investigation of the May 22, 2011, Tornado in Joplin, Missouri. National Institute of Standards and Technology (NIST); 2014.
[4] Wurman J, Randall M, Zahrai A. Design and deployment of a portable, pencil-beam, pulsed, 3-cm Doppler radar. J Atmos Ocean Technol 1997;14:1531–9.
[5] Hangan H, Kim J. Swirl ratio effects on tornado vortices in relation to the Fujita scale. Wind Struct 2008;11:291–302.
[6] Refan M, Hangan H, Wurman J. Reproducing tornadoes in laboratory using proper scaling. J Wind Eng Ind Aerodyn 2014;135:136–48.
[7] Lee WC, Jou JD, Chang PL, Deng SM. Tropical cyclone kinematic structure retrieved from single-Doppler radar observations. Part I: interpretation of Doppler velocity patterns and the GBVTD technique. Mon Weather Rev 1999;127:2419–39.
[8] Hangan H. The Wind Engineering Energy and Environment (WindEEE) Dome at Western University, Canada. Wind Eng JAWE 2014;39:350–1.
[9] Wind Science and Engineering Centre. A Recommendation for an Enhanced Fujita scale (EF-Scale). Texas Tech University; 2004.
[10] Ward NB. The exploration of certain features of tornado dynamics using a laboratory model. J Atmos Sci 1972;29:1194–204.
[11] Davies-Jones RP. The dependence of core radius on swirl ratio in a tornado simulator. J Atmos Sci 1973;30:1427–30.
[12] Davies-Jones RP. Laboratory simulations of tornadoes. In: Proc. Symp. Tornadoes Assess. Knowl. Implic. Man, Lubbock, TX: Texas Tech University; 1976, p. 151–74.
[13] Church CR, Snow JT, Baker GL, Agee EM. Characteristics of tornado-like vortices as a function of swirl ratio: a laboratory investigation. J Atmos Sci 1979;36:1155–76.
[14] Snow JT. A review of recent advances in tornado vortex dynamics. Rev Geophys 1982;20:953–64.
[15] Rotunno RA. A study in tornado-like vortex dynamics. J Atmos Sci 1979;36:140–55.
[16] Lewellen WS, Sheng YP. Influence of surface conditions on tornado wind distribution. Bull Am Meteorol Soc 1979;60. 525–525.
[17] Lewellen DC, Lewellen WS, Xia J. The influence of a local swirl ratio on tornado intensification near the surface. J Atmos Sci 2000;57:527–44.
[18] Kuai L, Haan FL, Gallus WA, Sarkar PP. CFD simulations of the flow field of a laboratory-simulated tornado for parameter sensitivity studies and comparison with field measurements. Wind Struct 2008;11:1–22.
[19] Davies-Jones RR, Trapp J, Bluestein HB. Tornadoes and tornadic storms. Meteorol Monogr 2001;28:167–222. http://dx.doi.org/10.1175/0065-9401-28.50.167.
[20] Hall MG. The structure of concentrated vortex cores. Prog Aerosp Sci 1966;7:53–6.
[21] Hall MG. Vortex breakdown. Annu Rev Fluid Mech 1972;4:195–218. http://dx.doi.org/10.1146/annurev.fl.04.010172.001211.
[22] Pauley RL, Snow JT. On the kinematics and dynamics of the 18 July 1986 Minneapolis tornado. Mon Weather Rev 1989;116:2731–6.
[23] Lugt HJ. Vortex breakdown in atmospheric columnar vortices. Bull Amer Meteor Soc 1989;70:1526–37.
[24] Pauley RL, Church CR, Snow JT. Measurements of maximum surface pressure deficits in modeled atmospheric vortices. J Atmos Sci 1982;39:368–77.
[25] Wurman J. The DOW mobile multiple-Doppler network. Munich, Germany: Amer. Meteor. Soc.; 2001. p. 95–7.
[26] Rasmussen EN, Straka JM, Davies-Jones R, Doswell III CA, Carr FH, Eilts MD, et al. Verification of the origins of rotation in tornadoes experiment: VORTEX. Bull Am Meteor Soc 1994;75:995–1006.
[27] Wurman J, Straka J, Rasmussen E. Fine scale Doppler radar observation of tornadoes. Science 1996;272:1774–7.
[28] Wurman J, Gill S. Fine-scale radar observations of the Dimmitt, Texas (2 June 1995) tornado. Mon Weather Rev 2000;128:2135–64.
[29] Dowell DC, Bluestein HB. The 8 June 1995 McLean, Texas, storm. Part I: observations of cyclic tornadogenesis. Mon Weather Rev 2002;130:2626–48. http://dx.doi.org/10.1175/1520-0493(2002) 130<2626:TJMTSP>2.0.CO;2.
[30] Wurman J. Preliminary results from the ROTATE-98 tornado experiment. Am Meteor Soc 1998:120–3.
[31] Wurman J. Multiple-Doppler observations of tornadoes and tornadogenesis during the ROTATE-2003 project. Am Meteor Soc 2003.
[32] Wurman J, Richardson Y, Alexander C, Weygandt S, Zhang PF. Dual-Doppler analysis of winds and vorticity budget terms near a tornado. Mon Weather Rev 2007;135:2392–405. http://dx.doi.org/10.1175/MWR3404.1.
[33] Wurman J. The multiple-vortex structure of a tornado. Am Meteorol Soc 2002;17:473–505.
[34] Alexander CR, Wurman J. The 30 May 1998 Spencer, South Dakota, storm, Part I: the structural evolution and environment of the tornadoes. Mon Weather Rev 2005;133:72–97. http://dx.doi.org/10.1175/MWR-2855.1.
[35] Lee WC, Wurman J. Diagnosed three-dimensional axisymmetric structure of the Mulhall tornado on 3 May 1999. J Atmos Sci 2005;62:2373–93.
[36] Kosiba K, Trapp J, Wurman J. An analysis of the axisymmetric three-dimensional low level wind field in a tornado using mobile radar observations. Geophys Res Lett 2008;35:1–6.
[37] Kosiba K, Wurman J. The three-dimensional axisymmetric wind field structure of the Spencer, South Dakota, 1998 tornado. J Atmos Sci 2010;67:3074–83.
[38] Wurman J, Alexander C, Robinson P. Low level winds in tornadoes and potential catastrophic tornado impacts in urban areas. Bull Am Meteor Soc 2007;88:31–46.
[39] Burgess DW, Magsig MA, Wurman J, Dowell DC, Richardson Y. Radar observations of the 3 May 1999 Oklahoma City tornado. Weather Forecast 2002;17:456–71. http://dx.doi.org/10.1175/1520-0434(2002) 017<0456:ROTMO>2.0.CO;2.
[40] Wurman J, Alexander CR. The 30 May 1998 Spencer, South Dakota, storm. Part II: comparison of observed damage and radar-derived winds in the tornadoes. Mon Weather Rev 2005;133:97–119.
[41] Kosiba K, Wurman J. The three-dimensional structure and evolution of a tornado boundary layer. Weather Forecast 2013;28:1552–61.
[42] Tanamachi RL, Bluestein HB, Lee W-C, Bell M, Pazmany A. Ground-Based Velocity Track Display (GBVTD) analysis of W-Band Doppler radar data in a tornado near Stockton, Kansas, on 15 May 1999. Mon Weather Rev 2007;135:783–800. http://dx.doi.org/10.1175/MWR3325.1.
[43] Bluestein HB, Weiss CC, French MM, Holthaus EM, Tanamachi RL, Frasier S, et al. The structure of tornadoes near Attica, Kansas, on 12 May 2004: High-resolution, mobile, Doppler radar observations. Mon Weather Rev 2007;135:475–506. http://dx.doi.org/10.1175/MWR3295.1.
[44] Wakimoto RM, Stauffer P, Lee WC, Atkins NT, Wurman J. Finescale structure of the LaGrange, Wyoming tornado during VORTEX2: GBVTD and photogrammetric analyses. Mon Weather Rev 2012;140:3397–418.
[45] Wurman J, Kosiba K, Robinson P, Marshall T. The role of multiple-vortex tornado structure in causing storm researcher fatalities. Bull Am Meteorol Soc 2013;95:31–45. http://dx.doi.org/10.1175/BAMS-D-13-00221.1.
[46] Wurman J, Kosiba K, Robinson P. In situ, Doppler radar, and video observations of the interior structure of a tornado and the wind damage relationship. Bull Am Meteorol Soc 2013;94:835–46. http://dx.doi.org/10.1175/BAMS-D-12-00114.1.
[47] Nolan DS. On the use of Doppler-radar-derived wind fields to diagnose the secondary circulation of tornadoes. J Atmos Sci 2013;70:1160–71.
[48] Dowell DC, Alexander CR, Wurman JM, Wicker LJ. Centrifuging of hydrometeors and debris in tornadoes: radar-reflectivity patterns and wind-measurement errors. Mon Weather Rev 2005;133:1501–24. http://dx.doi.org/10.1175/MWR2934.1.
[49] Mohr CG, Jay Miller L, Vaughan RL, Frank HW. The merger of mesoscale datasets into a common Cartesian format for efficient and systematic analyses. J Atmos Ocean Technol 1986;3:143–61. http://dx.doi.org/10.1175/1520-0426(1986) 003<0143:TMOMDI >2.0.CO;2.
[50] Wood VT, Brown RA. Effects of radar proximity on single-Doppler velocity signatures of axisymmetric rotation and divergence. Mon Weather Rev

1992;120:2798–807. http://dx.doi.org/10.1175/1520-0493(1992)120<2798:EORPOS>2.0.CO;2.
[51] Oye R, Mueller C, Smith C. Software for radar translation, visualization, editing, and interpolation. Am Meteor Soc 1995:259–361.
[52] Kepert J. The dynamics of boundary layer jets within the tropical cyclone core. Part I: linear theory. J Atmos Sci 2001;58:2469–84. http://dx.doi.org/10.1175/1520-0469(2001)058<2469:TDOBLJ>2.0.CO;2.
[53] Trapp RJ, Doswell CA. Radar data objective analysis. J Atmos Ocean Technol 2000;17:105–20. http://dx.doi.org/10.1175/1520-0426(2000)017<0105:RDOA>2.0.CO;2.
[54] Majcen M, Markowski P, Richardson Y, Dowell D, Wurman J. Multipass objective analyses of Doppler radar data. J Atmos Ocean Technol 2008;25:1845–58. http://dx.doi.org/10.1175/2008JTECHA1089.1.
[55] Markowski P, Richardson Y, Marquis J, Wurman J, Kosiba K, Robinson P, et al. The pretornadic phase of the Goshen County, Wyoming, supercell of 5 June 2009 intercepted by VORTEX2. Part I: evolution of kinematic and surface thermodynamic fields. Mon Weather Rev 2012;140:2887–915. http://dx.doi.org/10.1175/MWR-D-11-00336.1.
[56] Markowski P, Richardson Y, Marquis J, Davies-Jones R, Wurman J, Kosiba K, et al. The pretornadic phase of the Goshen County, Wyoming, supercell of 5 June 2009 intercepted by VORTEX2. Part II: Intensification of low-level rotation. Mon Weather Rev 2012;140:2916–38. http://dx.doi.org/10.1175/MWR-D-11-00337.1.
[57] Kosiba K, Wurman J, Richardson Y, Markowski P, Robinson P, Marquis J. Genesis of the Goshen County, Wyoming, tornado on 5 June 2009 during VORTEX2. Mon Weather Rev 2013;141:1157–81. http://dx.doi.org/10.1175/MWR-D-12-00056.1.
[58] Marquis J, Richardson Y, Markowski P, Dowell D, Wurman J, Kosiba K, et al. An investigation of the Goshen County, Wyoming, tornadic supercell of 5 June 2009 using EnKF assimilation of mobile mesonet and radar observations collected during VORTEX2. Part I: experiment design and verification of the EnKF analyses. Mon Weather Rev 2014;142:530–54. http://dx.doi.org/10.1175/MWR-D-13-00007.1.
[59] Fiedler BH, Rotunno R. A theory for the maximum wind speeds in tornado-like vortices. J Atmos Sci 1986;43:2328–40. http://dx.doi.org/10.1175/1520-0469(1986)043<2328:ATOTMW>2.0.CO;2.
[60] Houston SH, Powell MD. Observed and modeled wind and water-level response from tropical storm Marco (1990). Weather Forecast 1994;9:427–39. http://dx.doi.org/10.1175/1520-0434(1994)009<0427:OAMWAW>2.0.CO;2.
[61] Depperman CE. Notes on the origin and structure of Philippine typhoons. Bull Am Meteorol Soc 1947;28:399–404.
[62] Snow JT. On the formation of particle sheaths in columnar vortices. J Atmos Sci 1984;41:2477–91.
[63] Refan M, Hangan H, Siddiqui K. Particle image velocimetry measurements of tornado-like flow field in Model WindEEE Dome, ASME; 2014.
[64] Natarajan D. Numerical simulation of tornado-like vortices; 2011.
[65] Natarajan D, Hangan H. Large eddy simulations of translation and surface roughness effects on tornado-like vortices. J Wind Eng Ind Aerodyn 2012;104–106:577–84.
[66] Church CR, Snow JT, Agee EM. Tornado vortex simulation at Purdue University. Bull Am Meteorol Soc 1977;58:900–8.
[67] Hashemi Tari P, Gurka R, Hangan H. Experimental investigation of a tornado-like vortex dynamics with swirl ratio: the mean and turbulent flow fields. J Wind Eng Ind Aerodyn 2010;98:936–44.
[68] Refan M, Hangan H. Characterization of tornado-like flow fields in a new model scale wind testing chamber. J Wind Eng Ind Aerodyn 2016;151:107–21.